

RESEARCH

In vitro cone beam computed tomography imaging of periodontal bone

A Mol*¹ and A Balasundaram²

¹Department of Diagnostic Sciences and General Dentistry, School of Dentistry, The University of North Carolina at Chapel Hill, Chapel Hill, North Carolina, USA; ²Department of Diagnostic Sciences, School of Dentistry, University of Detroit Mercy, Detroit, Michigan, USA

Objectives: To assess the accuracy of NewTom 9000 cone beam CT (CBCT) images for the detection and quantification of periodontal bone defects in three dimensions.

Methods: A sample of 146 sites in 5 dry skulls provided the ground truth (GT). Half of the sample had bone loss of at least 3 mm. Two metal spheres at each site ensured correspondence between GT and CBCT measurements. Skulls were submerged in water and scanned with the NewTom QR-DVT-9000. A full mouth series (FMX) was obtained of each skull using photostimulable phosphor plates. Six observers measured the bone height of each site and rated the presence or absence of bone loss. Measurements were compared to GT and A_z -values were calculated from receiver operating characteristic curves.

Results: The A_z -value for CBCT was 0.74 (standard deviation (SD) = 0.14) and for FMX 0.48 (SD = 0.09). The difference was significant (ANOVA: $P < 0.01$). The diagnostic accuracy of CBCT was lower for anterior teeth ($A_z = 0.59$) than for molars ($A_z = 0.82$) and premolars ($A_z = 0.79$) (Tukey's HSD (honestly significant difference): $P < 0.01$). The mean absolute difference between CBCT and GT was 1.27 mm (SD = 1.43) and between FMX and GT 1.49 mm (SE = 1.24) (ANOVA: $P < 0.01$). Measurements in the anterior mandible were less accurate than in other areas (Tukey's HSD: $P < 0.01$).

Conclusion: The NewTom 9000 cone beam CT scanner provides better diagnostic and quantitative information on periodontal bone levels in three dimensions than conventional radiography. The accuracy in the anterior aspect of the jaws is limited.

Dentomaxillofacial Radiology (2008) **37**, 319–324. doi: 10.1259/dmfr/26475758

Keywords: radiography, dental; computed tomography, X-ray; alveolar bone loss

Introduction

Two basic elements of a periodontal diagnosis are the severity of the problem and whether the condition is localized or generalized.¹ Radiography plays an important adjunctive role in periodontal diagnosis, primarily by providing information regarding the amount and type of damage to the alveolar bone.^{1,2} While radiographs also reveal related issues, such as calculus and defective restorations, assessment of alveolar bone height with respect to the cemento-enamel junction is the main outcome of a radiological examination in support of a periodontal diagnosis.

Conventional modalities commonly used for assessing alveolar bone height include bitewing, periapical and panoramic radiography.^{2–5} The bitewing technique is the conventional modality that is best suited for assessing bone height, because it approaches ideal projection geometry and shows both mandibular and maxillary structures.^{2,6–8} However, all conventional modalities produce two-dimensional images that collapse the three-dimensional structures based on differential attenuation of X-rays. Thus, important aspects of the alveolar bone may go undetected as a result of an unfavourable location with respect to other structures or an unfavourable orientation with respect to the X-ray beam. Only the interproximal bone levels can be detected with some level of certainty.² Even when high-quality images are produced, intraoral radiographs

*Correspondence to: Dr André Mol, Department of Diagnostic Sciences and General Dentistry, UNC School of Dentistry, CB 7450, Chapel Hill, NC 27599–7450; E-mail: mola@dentistry.unc.edu
Received 4 October 2007; revised 20 November 2007; accepted 24 November 2007

have been shown to underestimate mild to moderate bone loss.^{3,9–11}

Subtraction radiography, by virtue of its highly standardized acquisition technique and precise analytical methods, has been shown to be more accurate and to allow for earlier detection of osseous changes than conventional radiography.^{12–14} However, this technique is labour intensive and does not have the capability to provide accurate three-dimensional (3D) information either. The inherent limitations of conventional radiography result in incomplete and imprecise assessment of the condition of the alveolar bone.

The ability to visualize the alveolar bone in 3D and make measurements at any location has the potential to significantly improve periodontal diagnosis. The modality that is best suited for 3D imaging of mineralized tissues is CT. Studies have shown that assessment of alveolar bone height on CT images is reasonably accurate and precise. However, medical CT examinations are dose intense and have an unfavourable cost-benefit ratio for periodontal purposes.

These drawbacks have largely been overcome with the development of cone beam CT (CBCT) scanners. CBCT scanners are specifically designed for imaging the hard tissues of the head and neck. They are much cheaper than medical CT units, impart a relatively low dose to the patient¹⁵ and are becoming rapidly available to the dental profession. It is the purpose of this study to assess the usefulness of CBCT for the assessment of alveolar bone loss and compare its diagnostic performance with periapical and bitewing radiography *in vitro*. The specific aims of this study are to assess the diagnostic efficacy of NewTom 9000 CBCT images for the detection of alveolar bone loss and to determine the accuracy of quantitative measurements of alveolar bone height in 3D.

Materials and methods

Five dentate dry skulls were selected to provide the periodontal ground truth (GT) model. The sample consisted of 146 sites stratified according to tooth group and site location. Six tooth groups were identified: upper molar (UM), upper premolar (UP),

upper anterior (UA), lower molar (LM), lower premolar (LP) and lower anterior (LA). The actual measurement sites were classified as mesiobuccal (MB), buccal (B), distobuccal (DB), mesiolingual (ML), lingual (L) and distolingual (DL). Based on a bone loss threshold of 3 mm, half of the sample was “healthy” (median = 2.4 mm; interquartile range (IQR) = 0.5 mm) and the other half showed bone loss (median = 4.2 mm; IQR = 1.3 mm). Table 1 shows the distribution of the sites per tooth group and site location.

Two small metal spheres were attached to the crown of the tooth at each site to mark the exact location and orientation of each measurement. Measurement of the distance between the cemento-enamel junction and the alveolar crest was performed according to the line connecting the spheres. Skull measurements were made by a single examiner (AB) using a digital caliper with a resolving capacity of 0.1 mm. The average of three measurements was considered the GT value.

Image acquisition

The skulls were scanned with the NewTom QR-DVT-9000 CBCT unit (QR-NIM s.r.l., Verona, Italy). Scans were performed with the skulls submerged in water to provide adequate X-ray attenuation and scattering. Exposure parameters were selected automatically by the scanner based on the attenuation properties of each skull. Primary reconstruction of the raw data resulted in axial slices parallel to the occlusal plane with a slice thickness of 0.3 mm. For those skulls that exhibited a deep curve of Spee, multiple primary reconstructions were performed to yield axial images that were locally parallel to the occlusal plane for each region of interest.

Cross-sectional slices of 1 mm thickness were constructed from the axial slices for each site. The slice location and orientation was dictated by the metallic markers such that both markers were visible in the slice (Figure 1). This ensured correspondence between slice measurements and ground truth measurements.

A series of 14 periapical and 4 vertical bitewing radiographs (FMX) was obtained of each skull using photostimulable phosphor (PSP) plates. The plates were scanned with the Gendex DenOptix scanner at 300 dots per inch and stored as 8-bit Joint Photographic

Table 1 Distribution of sample sites by tooth group, site location and amount of bone loss

	<3 mm							≥3 mm						
	MB	B	DB	DL	L	ML	total	MB	B	DB	DL	L	ML	total
LA	0	5	4	2	1	0	12	0	5	4	0	3	0	12
LM	0	8	3	1	0	0	12	2	2	3	0	3	1	11
LP	0	8	4	0	0	0	12	3	3	2	0	3	1	12
UA	0	5	2	3	2	0	12	0	8	4	1	1	0	14
UM	0	9	3	0	0	0	12	0	2	3	3	4	0	12
UP	0	9	3	0	1	0	13	1	5	2	1	3	0	12
total	0	44	19	6	4	0	73	6	25	18	5	17	2	73
% total	0.0	60.3	26.0	8.2	5.5	0.0	100.0	8.2	34.2	24.7	6.8	23.3	2.7	100.0

B, buccal; DB, distobuccal; DL, distolingual; L, lingual; LA, lower anterior; LM, lower molar; LP, lower premolar; MB, mesiobuccal; ML, mesiolingual; UA, upper anterior; UM, upper molar; UP, upper premolar

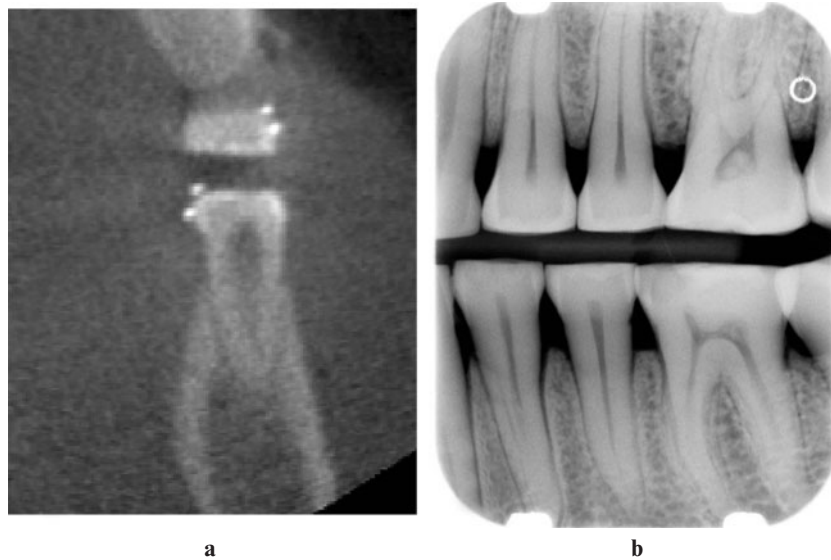


Figure 1 (a) Cross-sectional cone beam CT slice through the mandibular left first premolar. The two metal spheres on the lingual surface mark the area of interest. (b) Corresponding bitewing radiograph

Experts Group File Interchange Format (JFIF) images at maximum quality (100%).

Image viewing

CBCT image slices were exported from the NewTom software in bitmap format. Gendex PSP images were exported in JPEG (Joint Photographic Experts Group) format. Images from both modalities were then imported into Schick CDR software (Schick Technologies, Inc., Long Island City, NY). Both sets of images were spatially calibrated according to known dimensions of the native images. A magnification factor of 1.05 was used for all intraoral images.

Four board-certified oral and maxillofacial radiologists, one oral and maxillofacial radiology resident and one periodontist were recruited as observers. The observers were calibrated using a training session. The observers were asked to measure the distance between the cemento-enamel junction and the alveolar crest for each site and each modality using the Schick CDR length measurement tool. Based on a bone loss threshold of 3 mm, they were also asked to assess the presence or absence of bone loss (vertical or horizontal) on a five-point scale as follows: 1 = bone loss definitely absent, 2 = bone loss probably absent, 3 = uncertain, 4 = bone loss probably present, 5 = bone loss definitely present.

The observations were performed in seven separate sessions: three CBCT sessions, three FMX sessions and one combined CBCT-FMX repeat session. The order in which the two modalities were viewed was reversed for half of the observers to minimize order effects. The presentation of the images within and among sessions was random. The repeat session included a 20% random sample from the main sessions.

Data analysis

CBCT and FMX measurements were compared to GT measurements using ANOVA statistics. Since positive and negative differences cancel each other out, analysis was performed on the absolute differences. Actual differences were considered only to determine the direction of the differences. The main effects of modality, tooth group, site and observer were tested along with the interactions. Tukey's HSD (honestly significant difference) *post hoc* test was used to determine significant differences within groups.

Diagnostic accuracy of determining the presence or absence of bone loss was assessed using receiver operating characteristic (ROC) curves. The area under the curve (A_z) was calculated for each combination of observer, modality and tooth group using ROCKIT 0.9B (Charles Metz, University of Chicago, Chicago, IL). Differences between areas under the curves (A_z) were analysed using ANOVA ($\alpha = 0.05$).

Intraobserver agreement for bone loss assessment was determined by comparing ROC scores of repeated observations. The kappa statistic with linear weighting was used to account for chance agreement (VassarStats; Richard Lowry, Vassar College, Poughkeepsie, NY).

Results

The results of the ROC analysis are presented in Table 2 and Figures 2-4. Analysis by tooth group resulted in degenerate data making it necessary to collapse the original six tooth groups into three (molars, premolars and anterior teeth). ANOVA showed that differences between observers were not statistically significant ($P = 0.69$), but differences

Table 2 Bone loss detection accuracy as measured by A_z (receiver operating characteristics analysis) for each modality and tooth group. Homogeneous subsets for all data based on Tukey's HSD (honestly significant difference) *post hoc* test

Modality	Tooth group	Mean A_z	SD	Homogeneous subsets
CBCT	Molar	0.82	0.14	A
	Premolar	0.79	0.07	A
	Anterior	0.59	0.06	B
FMX	Molar	0.45	0.06	B
	Premolar	0.52	0.11	B
	Anterior	0.46	0.08	B

CBCT, cone beam CT; FMX, full-mouth series; SD, standard deviation

between modalities ($P < 0.0001$), tooth groups ($P = 0.01$) and the interaction between modality and tooth group ($P = 0.01$) were. Tukey's HSD *post hoc* test showed that CBCT was significantly better than FMX for the molar and premolar tooth groups. The diagnostic accuracy of CBCT in the anterior region was not significantly different from the diagnostic accuracy of FMX.

The average difference between GT measurements and CBCT measurements was -0.23 mm. This implies that there was slightly more underestimation than overestimation of bone loss. For FMX, the average actual difference was -1.17 mm, also implying more underestimation than overestimation of bone loss. The real difference between GT measurements and image measurements is better described by the absolute difference. While this measure does not account for the direction of the error, it prevents positive and negative errors from cancelling each other out. Absolute differences between GT measurements and measurements

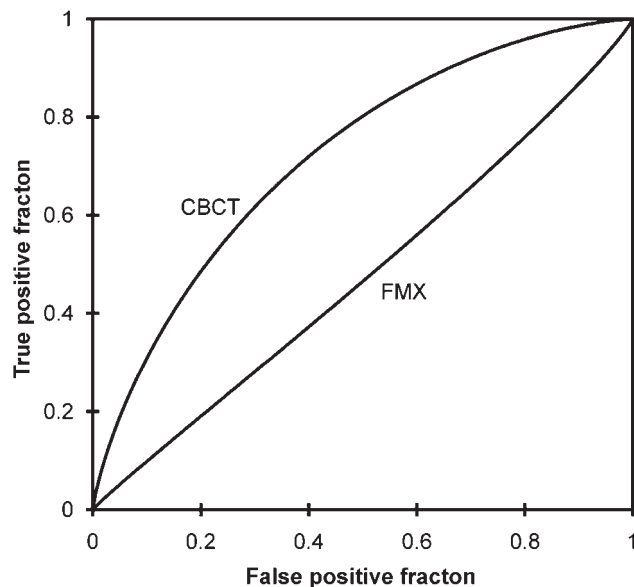


Figure 2 Receiver operating characteristic curves of pooled data from all observers for cone-beam CT (CBCT) and full-mouth series (FMX)

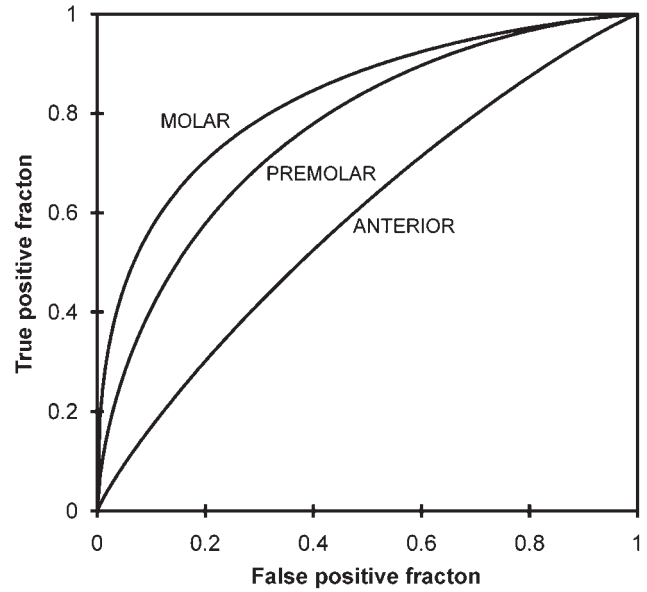


Figure 3 Receiver operating characteristic curves of pooled data from all observers for cone beam CT by tooth group

from either of the two imaging modalities are summarized in Table 3. Overall, CBCT measurements were more accurate than FMX measurements ($P < 0.0001$). There was no significant difference between observers. Tooth group differences were significant ($P < 0.0001$). Table 3 also shows the homogeneous subsets based on Tukey's *post hoc* test. The measurement error for the LA teeth was significantly larger than for the other tooth groups for both modalities. The interaction between modality and tooth group was not statistically significant.

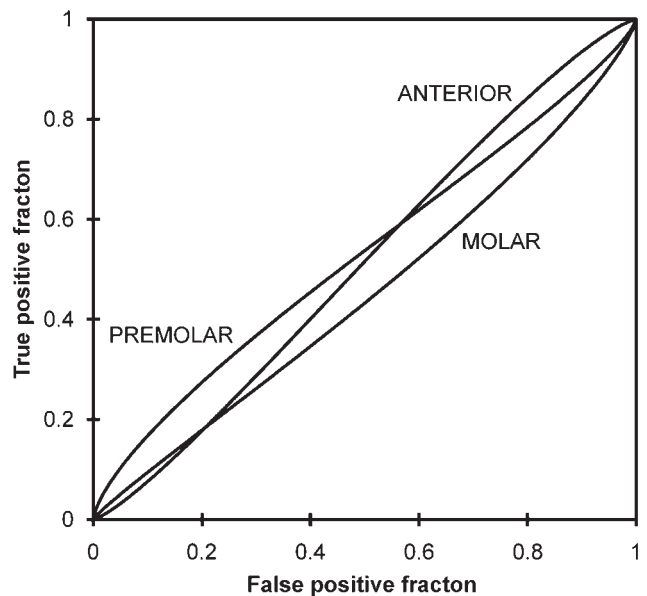


Figure 4 Receiver operating characteristic curves of pooled data from all observers for full-mouth series by tooth group

Table 3 Absolute differences between ground truth measurements and image measurements by modality and tooth group. Homogeneous subsets by modality based on Tukey's HSD (honestly significant difference) *post hoc* test

		UM	UP	UA	LM	LP	LA	Pooled
CBCT	Mean	1.14	0.91	1.46	1.00	1.16	1.95	1.27
	SD	1.38	0.75	1.63	1.11	1.31	1.89	1.43
Homogeneous subsets		A,B	A	B	A,B	A,B	C	
FMX	Mean	1.38	1.22	1.48	1.16	1.48	2.24	1.49
	SD	0.98	0.91	1.24	0.98	1.11	1.78	1.24
Homogeneous subsets		A	A	A	A	A	B	

CBCT, cone beam computed tomography; FMX, full-mouth series; LM, lower molar; LP, lower premolar; SD, standard deviation; UA, upper anterior; UM, upper molar; UP, upper premolar

Kappa values representing intraobserver agreement for bone loss assessment are shown in Table 4. Overall, both modalities resulted in slight agreement, with only two observers showing fair agreement.¹⁶

Discussion

The purpose of this study was to assess the usefulness of CBCT for the assessment of alveolar bone loss and compare its diagnostic performance with periapical and bitewing radiography. The results show that the accuracy of detecting bone loss was significantly better with CBCT than with conventional intraoral radiographs. This was true only for posterior teeth. The diagnostic accuracy of both imaging modalities was low for anterior teeth. The difference in the diagnostic accuracy of CBCT between anterior and posterior teeth is likely the result of the difference in the morphology of the periodontal bone between these areas. The buccal and lingual plates are considerably thinner in the anterior region and the bone tapers towards the crest. Apparently, the quality of the CBCT image slices is insufficient to resolve the alveolar crest reliably in this region.

The inclusion of buccal and lingual sites in the sample created a bias in favour of CBCT as it is known that bone levels in these areas are very difficult to visualize with intraoral radiographs. The inclusion of these sites demonstrated the capability of 3D imaging to visualize bone levels in areas where conventional modalities fall short. The sample was somewhat unbalanced because of the relatively large number of buccal sites. It should also be noted that the bias against conventional radiography was further increased by the fact that proximal sites were not absolutely mesial or distal. The selection of these sites was dictated by the need to obtain reliable ground truth measurements without destroying the sample. Considering these limitations, conventional radiography simply served as a control, confirming that 3D information cannot be obtained with traditional means.

Despite the higher diagnostic accuracy of CBCT, bone height measurements were only slightly better than those for conventional radiography. Both modalities resulted

Table 4 Kappa values for intraobserver agreement between repeated receiver operating characteristics scores from bone loss assessment

Observer	CBCT	FMX
1	0.13	0.00
2	0.15	0.22
3	-0.17	-0.05
4	0.34	0.32
5	0.32	0.30
6	0.11	-0.05
Pooled	0.15	0.14

CBCT, cone beam computed tomography; FMX, full-mouth series

in average measurement errors larger than 1 mm. This appears a clinically significant error requiring improvement.

Whereas CBCT was better than conventional radiography both in terms of diagnostic and quantitative accuracy, it was by no means perfect. It is known that perception errors are inherent to human observations and decisions; however, the magnitude of the error in visual perception is modulated by image clarity. The CBCT scans used in this study sometimes lacked image clarity, which was especially apparent in areas where diagnostic decisions were determined by small details. Lack of image clarity can be the result of limited spatial resolution, limited contrast resolution, poor signal-to-noise ratio (SNR) or a combination of these. The voxel size of approximately 0.3 mm suggests that CBCT could be useful for periodontal imaging. However, the cemento-enamel junction and, in some instances, the coronal edge of the alveolar bone are defined by tapering structures, which may challenge the spatial resolution of the system. Apart from voxel size, spatial resolution is also modulated by SNR, which may have been a key factor limiting the detection rate.

It should be emphasised that current results were obtained with an early generation CBCT scanner, which is no longer available. Recent advances in CBCT technology suggest that the current scanners, including the NewTom 3G, are likely to exceed the results obtained in this study. Improvements include increased contrast resolution through higher bit depth (from 8 bits to 12 bits), better SNR and higher spatial resolution. These developments and the results of this study support further investigation of the usefulness of CBCT for periodontal diagnosis to increase accuracy and expand periodontal bone height assessment beyond the traditional mesial and distal locations.

From the results of this study it can be concluded that the NewTom 9000 cone beam CT scanner provides better diagnostic and quantitative information on periodontal bone levels than conventional radiography. The accuracy in the anterior aspect of the jaws is limited.

Acknowledgment

The authors wish to thank to Dr John Ludlow for his help with the statistical analyses.

References

1. Armitage GC. The complete periodontal examination. *Periodontol 2000* 2004; **34**: 22–33.
2. Mol A. Imaging methods in periodontology. *Periodontol 2000* 2004; **34**: 34–48.
3. Åkesson L, Håkansson J, Rohlin M. Comparison of panoramic and intraoral radiography and pocket probing for the measurement of the marginal bone level. *J Clin Periodontol* 1992; **19**: 326–332.
4. Jeffcoat M, Wang I, Reddy M. Radiographic diagnosis in periodontics. *Periodontol 2000* 1995; **7**: 54–68.
5. Tugnait A, Clerehugh V, Hirschmann P. The usefulness of radiographs in diagnosis and management of periodontal diseases: a review. *J Dent* 2000; **28**: 219–226.
6. Eley B, Cox S. Advances in periodontal diagnosis 1. Traditional clinical methods of diagnosis. *Br Dent J* 1998; **184**: 12–16.
7. Hausmann E. A contemporary perspective on techniques for the clinical assessment of alveolar bone. *J Periodontol* 1990; **61**: 149–156.
8. White S, Heslop E, Hollender L, Mosier K, Ruprecht A, Shrout M. Parameters of radiologic care: an official report of the Academy of Oral and Maxillofacial Radiology. *Oral Surg Oral Med Oral Pathol Oral Radiol Endod* 2001; **91**: 498–511.
9. Eickholz P, Hausmann E. Accuracy of radiographic assessment of interproximal bone loss in intrabony defects using linear measurements. *Eur J Oral Sci* 2000; **108**: 70–73.
10. Pepelassi E, Diamanti-Kipiotti A. Selection of the most accurate method of conventional radiography for the assessment of periodontal osseous destruction. *J Clin Periodontol* 1997; **24**: 557–567.
11. Tonetti M, Pini-Prato G, Williams R, Cortellini P. Periodontal regeneration of human infrabony defects: III. Diagnostic strategies to detect bone gain. *J Periodontol* 1993; **64**: 269–277.
12. Mol A, Dunn S. The performance of projective standardization for digital subtraction radiography. *Oral Surg Oral Med Oral Pathol Oral Radiol Endod* 2003; **96**: 373–382.
13. Ortman LF, Dunford R, McHenry K, Hausmann E. Subtraction radiography and computer assisted densitometric analyses of standardized radiographs. A comparison study with ¹²⁵I absorptiometry. *J Periodontol Res* 1985; **20**: 644–651.
14. Reddy MS, Jeffcoat MK. Digital subtraction radiography. *Dent Clin North Am* 1993; **37**: 553–565.
15. Ludlow JB, Davies-Ludlow LE, Brooks SL, Howerton WB. Dosimetry of 3 CBCT devices for oral and maxillofacial radiology: CB Mercuray, NewTom 3G and i-CAT. *Dentomaxillofac Radiol* 2006; **35**: 219–26.
16. Landis JR, Koch CG. The measurement of observer agreement for categorical data. *Biometrics* 1977; **33**: 159–174.